Study on Luteolysis Mechanisms via Lymphatic Vessels in Cow

March 2015

Hironori Abe

Graduate School of Environmental and Life Science
(Doctor's Course)

OKAYAMA UNIVERSITY

PREFACE

The experiments described in this dissertation were carried out at the Graduate School of Environmental and Life Science (Doctor's course), Okayama University, Japan, from April 2012 to March 2015, under the supervision of Professor Kiyoshi OKUDA.

This dissertation has not been submitted previously in whole or in part to a council, university or any other professional institution for a degree, diploma or other professional qualifications.

Hironori Abe

March, 2015

ACKOWLEDGMENTS

I wish to expresses my deep gratitude to Dr. Kiyoshi OKUDA, Professor at the Graduate School of Environmental and Life Science, Okayama University, Japan, for his guidance, encouragement, constructive criticism and excellent supervision and for providing me the opportunity to conduct this study. I also wish to thank Dr. Tomas J. ACOSTA and Dr. Yuki YAMAMOTO of Okayama University for their support, encouragement and advice at all stages of this study. It is pleasure to express my thanks to all members of the Laboratory of Animal Reproductive Physiology, who have helped me during this study.

CONTENTS

LIST OF FIGURES AND TABLES

ABSTRACT

Hironori ABE

Graduate School of Environmental and Life Science
OKAYAMA UNIVERSITY

In mammals, the corpus luteum (CL) is an essential endocrine gland for the establishment and maintenance of pregnancy. If pregnancy is not established, the CL regresses and disappears rapidly from the ovary (luteolysis). The number of the macrophages, which englobe apoptotic luteal cell, increases during luteolysis. However, during luteolysis induced by prostaglandin F2α (PGF) injection, the number of the macrophages observed in the CL does not increase compared with that observed in the CL in spontaneous luteolysis, although the time needed for disappearance of the CL from the ovary is shorter than that in spontaneous luteolysis. A possible explanation for the rapid disappearance of the CL is that luteal cells are transported from the ovary via lymphatic vessels. In the present study, we report the presence of cells positive for 3β-hydroxysteroid dehydrogenase (3β-HSD), an enzyme involved in progesterone synthesis, in the lumen of lymphatic vessels at the regressing luteal stage and in the lymphatic fluid collected from the ovarian pedicle ipsilateral to the regressing CL. The above findings strongly suggest that the 3β-HSD positive cells are luteal cells drained from the regressing CL. The 3β-HSD positive cells were alive and contained lipid droplets. The 3β-HSD positive cells in the lymphatic fluid were most abundant at days 22-24 after ovulation. These findings show that live steroidogenic cells are in the lymphatic vessels drained from the CL. The outflow of steroidogenic cells starts at the regressing luteal stage and continues after next ovulation.

Steroidogenic cells must be detached from the CL tissue in order that steroidogenic cells flow out to the lymphatic vessels. Matrix metalloproteinases (MMPs) are a family of proteolytic enzymes that has been reported to play important roles during the luteolytic process in cow. We hypothesized that luteolytic factors regulate the productions of MMPs in luteal cells during luteolysis, and that MMPs secreted by luteal cells break down the ECM surrounding luteal cells in the same way that MMPs secreted by cancer cells break down the ECM in metastasis. To test this hypothesis, we investigated the effects of three factors that are known to induce luteolysis (prostaglandin F2α (PGF), interferon γ (IFNG) and tumor necrosis factor α (TNF)) on the mRNA expressions of four MMPs involved in degrading collagen and

basal membrane in cultured luteal cell. Luteal cells obtained from the CL at the mid-luteal stage (days 8-12 after ovulation) were cultured with PGF (0.01, 0.1, 1 μM), IFNG (0.05, 0.5, 5 nM) and TNF (0.05, 0.5, 0.5 nM) alone or in combination for 24 h. PGF and IFNG significantly increased the MMP-1 mRNA. In addition, 1 μM PGF in combination with 5 nM IFNG stimulated MMP-1 and MMP-9 mRNA expression significantly more than did either treatment alone. In contrast, IFNG significantly decreased the levels of MMP-2 and MMP-14 mRNA. Five nM IFNG in combination with 5 nM TNF suppressed MMP-14 mRNA expression significantly more than did 5 nM IFNG alone. The above results suggest that PGF and IFNG are important factors regulating MMPs in luteal cells.

The overall findings suggest a novel luteolysis mechanism as follows:

1. PGF secreted by uterus, and IFNG secreted by macrophages that invade the CL, stimulate MMPs expression in bovine luteal cells.
2. The ECM surrounding luteal cells is degraded by MMPs secreted by luteal cells, and luteal cells are detached from the CL tissue, resulting in the outflow of luteal cells to the luteal lymphatic vessels.
3. The outflow of luteal cells is involved in the disappearance of the CL from the ovary.

CHAPTER 1
How luteal cells disappear from the corpus luteum in a short time during luteolysis in cow?

INTRODUCTION

In mammals, the corpus luteum (CL) formed after ovulation is an essential endocrine organ for the establishment and maintenance of pregnancy [1]. If pregnancy is not established, the CL regresses rapidly. The regression of the CL is essential to reset the ovarian cycle, so that mammals obtain another chance to become pregnant.

CL regression (luteolysis) consists of two phases, functional luteolysis and structural luteolysis [2]. Functional luteolysis is defined as declining in progesterone (P4) production. Structural luteolysis is characterized by a decrease in the volume of the CL due to loss of luteal cells. In cows, structural luteolysis is induced by uterine prostaglandin F2α (PGF2α), it takes 4–5 days to reduce the size of the CL [3]. This disappearance of CL tissue during structural luteolysis is generally explained by apoptosis of luteal cells and phagocytosis by intraluteal macrophages [2, 4, 5]. In agreement with this concept, the number of macrophages increases at the regressing luteal stage [6]. On the other hand, the volume of the CL decreases to less than half of its original size in 24 h after administration of PGF2α on Day 10 post ovulation [7]. However, the number of macrophages observed within the regressing CL during spontaneous and PGF2α-induced luteolysis is almost same [6]. Therefore, the mechanisms involved in the rapid disappearance of CL from the ovary have been a mystery for reproductive scientists.

The lymphatic vascular system, which is considered the body's second circulation system, is essential for transporting interstitial fluid, macromolecules (proteins, lipids) and cells [8]. The ovary has a rich network of lymphatic vessels. The lymphatic system has been suggested to be associated with folliculogenesis [9]. The CLs of primates and cows have lymphatic vessels [10, 11]. However, the function of the lymphatic vasculature in the CL is unclear.

In most human cancers, the lymphatic vasculature serves as the primary route for the metastatic spread of tumor cells to regional lymphatic nodes [8]. In a preliminary experiment, we found large lymphatic vessels near degenerated arterioles in the regressing CL. Therefore, we hypothesized that during structural luteolysis of bovine

CL, a large number of luteal cells flow out of the CL through the lymphatic vessels, similar to the flow of cancer cells in lymphatic vessels. The purpose of the present study was to test the above hypothesis. If confirmed, it could provide a novel explanation for the rapid decrease in size of the CL during structural lutolysis.

MATERIALS AND METHODS

Ethics Statement

In this study, we did not perform any animal experiments. The ovaries were collected from non-pregnant and pregnant (days 120-180 of pregnancy) Holstein cows at local abattoir (Tsuyama Meat Center) in accordance with protocols approved by local institutional animal care. The gestational ages were determined from fetal crown-rump length and classified as days 60-90 (6-20 cm), days 120-180 (25-45 cm) and days 210-270 (50-80 cm) [12]. All the samples and data analyzed in the present study were obtained with the permission of the above center.

Collection of ovary with CL and lymphatic fluid

The bovine CL and lymphatic fluid drained from the ovary were obtained from a local abattoir in accordance with protocols approved by the local institutional animal care and use committee. In cow, the ovulation occurs randomly in each ovary. Therefore, it is possible that the fresh and regressing CL are in a ovary, or also in each ovary. To identify the source of the cells in the lymphatic fluid, the lymphatic fluid was collected drained from a ovary with only a single CL. The CLs and lymphatic fluid samples were obtained within 30 min after exsanguination and were transported to the laboratory within 1-1.5 h on ice. In cows, ovulation generally occurs every 21 days. Luteal stages were classified as being early (Days 2–3 after ovulation), developing (Days 5-7), mid (Days 8–12), late (Days 15–17), regressing (Days 19-21) [13, 14]. The Days of previous CL were calculated based on the luteal stages of active CL on the contralateral ovary. For collecting the lymphatic fluid, the lymphatic vessels were, immediately after exsanguination ligated at 15 cm from ovarian hilus to allow accumulation of lymphatic fluid (Fig. 1B). Uterine blood and lymphatic vessels were cut immediately after ligation. Then, lymphatic vessels were dissected from connective tissue and lymphatic fluid accumulated in vessels was collected using a needle and syringe. To confirm that lymphatic vessels were drained from the CL, 2 ml of 0.1% Evans Blue staining solution was injected directly into the CL (Fig. 1).

Immunohistochemistry

CLs were fixed with 4% (v/v) paraformaldehyde (PFA) in PBS. 4 μm sections were mounted on glass slides pre-coated with silane (S3003; Dako, Glostrup, Denmark),

deparaffined and rehydrated. Antigen retrieval was achieved by Tris-EDTA buffer pH 9.0 using microwave for 15 min at 600 W. Sections were immersed in methanol with 3% (v/v) H2O2 for 30 min and incubated with 10% (v/v) normal horse serum (MP-7500; Vector Laboratories Inc, Burlingame, CA, USA) for blocking. Then, sections were incubated with LYVE-1 antibody (ab33682; abcam, Cambridge, UK) as a specific marker of lymphatic endothelial cells [10, 15, 16] diluted at 1:4000 with PBS for 1 h at room temperature (RT). Negative control sections were incubated with normal rabbit serum diluted by PBS. Subsequently, sections were incubated with ImmPRESS UNIVERSAL reagent, anti-mouse/rabbit Ig (MP-7500; Vector Laboratories Inc, Burlingame, CA, USA) for 30 min according to the manufacturer's instructions. The staining was visualized with 0.05% (w/v) 3,3'-diaminobenzidine (343-00901; Dojindo, Kumamoto, Japan) containing 0.01% (v/v) H2O2 and then counter-stained with hematoxylin. Bright field images were captured using FSX100 (Olympus, Tokyo, Japan) and merged using cellSens (Olympus, Tokyo, Japan).

Double Fluorescent Immunohistochemistry

4 μm sections were mounted on glass slides pre-coated with silane, deparaffined and rehydrated. Antigen retrieval was achieved by Tris-EDTA buffer pH 9 using microwave for 15 min at 600 W then sections were incubated with 10% (v/v) normal horse serum for blocking. Sections were incubated with LYVE-1 antibody diluted at 1:2000 with PBS and 3β-HSD antibody (ab75710; Abcam, Cambridge, UK) as a steroidogenic cell marker diluted 1:1000 with PBS for 1 h at RT. Negative control sections were incubated with normal rabbit serum and normal mouse serum diluted by PBS. Subsequently, the sections were incubated with Alexa Fluor 488 goat anti-rabbit IgG antibody (A-11008; Life Technologies, Carlsbad, CA, USA) and Alexa Fluor 594 goat anti-mouse IgG antibody (A-11005 Life Technologies, Carlsbad, CA, USA) for 1 h at RT. Nuclei were visualized using ProLong Gold including DAPI (P36935; Life Technologies, Carlsbad, CA, USA). Fluorescent images were captured using FSX100 and merged using cellSens (Olympus, Tokyo, Japan).

Smear of lymphatic fluid and staining

To determine the viability of cells found in the lymphatic fluid, trypan blue solution was diluted in lymphatic fluid to 0.12% finally. Immediately, the cells in the lymphatic fluid were observed using light field microscope. The smears of the

lymphatic fluid for each staining were performed according to the general biopsy manual. The lymphatic fluids smeared on glass slides pre-coated with silane were dried immediately and rehydrated with PBS. Subsequently the smears were dipped in 4% (v/v) PFA in PBS for 10 min at RT.

For fluorescent staining, the smears were incubated in 0.1% triton X-100 solution for 5 min. To inhibit non-specific staining, the smears were incubated with 10% (v/v) normal horse serum for 30 min. To demonstrate the presence of luteal cells in lymphatic fluid, the smear was incubated with 3β-HSD antibody diluted at 1:500 with PBS for 30 min at RT. Then the smear was incubated with Alexa Fluor 488 Goat anti-mouse IgG (A-11001; Life Technologies, Carlsbad, CA, USA) diluted at 1:1000 with PBS for 30 min at RT. The smear was incubated with Bodipy 493/503 (D-3922; Life Technologies, Carlsbad, CA, USA) used for lipid droplets-staining [17] diluted at 1:200 with PBS for 20 min at RT. Nuclei of all cells in smear were visualized using ProLong Gold including DAPI (P36935; Life Technologies, Carlsbad, CA, USA)then examined using FSX100. In this staining, bovine uterine stromal cultured cells were used as negative control.

Quantification of luteal cells in lymphatic fluid

To calculate the ratio of luteal cells to the whole cells in lymphatic fluid smear, 3 fields per a smear were selected randomly. The cells positively immunostained with 3β-HSD antibody and DAPI nuclear staining coinciding were counted by three independent observers. The percentage of the luteal cells in lymphatic fluid was calculated as $X/Y \times 100$, where X was the total number of immunostaining positive cells and Y was the total number of DAPI positive cells in the fields selected.

Statistical analysis

The statistical significance of differences in percentage of luteal cells in lymphatic fluids were assessed by analysis of variance (ANOVA) followed by a Fisher protected least significant difference procedure (PLSD) as a multiple comparison test and Bonferroni correction.

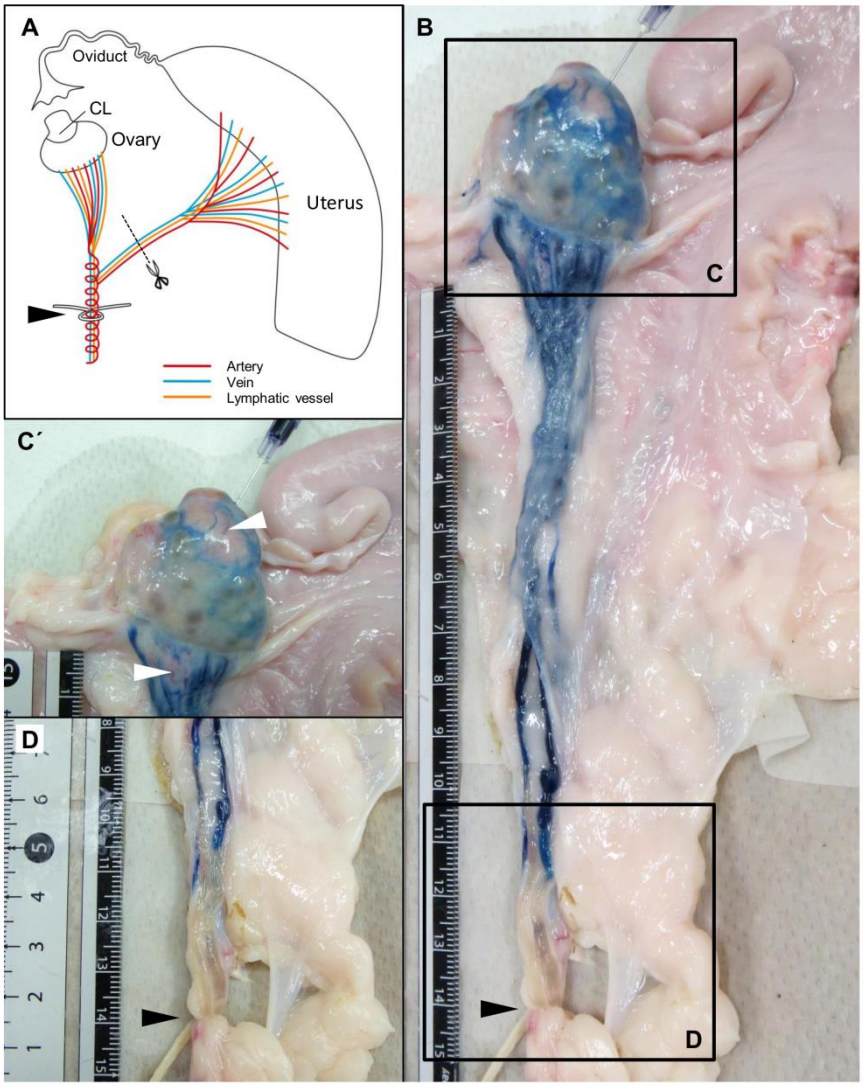

Figure 1. Anatomy of the ovarian lymphatic vessels.

A: The broad ligament has at least two lymphatic routes, one from the ovary and the other from the uterus. To collect lymphatic fluids, the lymphatic vessels were ligated at 15 cm distal to the ovary (black arrowhead). To avoid mixing ovarian and uterine lymphatic fluids, the lymphatic vessel draining the uterus was cut. B: To confirm that the collected lymphatic fluid was drained from the CL, 2 ml of 0.1% Evans Blue (EB) solution was injected into the CL (C). C: EB injected into the CL drained via lymphatic vessels (D). C´: EB was not observed in blood vessels (white arrowheads). D: The lymphatic fluid pooled in the lymphatic vessels was aspirated using a needle and syringe. Black arrowhead shows the ligation point.

RESULTS

Localization of lymphatic vessels and steroidogenic cells

In the regressing CL, large lymphatic vessels were detected near arterioles by staining with LYVE-1 antibody (Fig. 2A). Many 3β-HSD positive cells were found in the lumen of lymphatic vessels (Fig. 2E). LYVE-1 antibody reacted with 3β-HSD positive cells (Figs. 2C, D and E).

Characterization of cells in the lymphatic fluid

The volumes of lymphatic fluid collected from lymphatic vessels ranged from 10 to 200 μl. Most lymphatic fluid was accumulated within 15 min after ligation. The color of the fluid was variously as clear and yellow. Many yellow cells were found in the lymphatic fluid (Fig. 3A). Their sizes of those cells were about 20 μm and granules were observed in the cytoplasm (Fig. 3G). The yellow cells positively reacted with Bodipy (493/503) and 3β-HSD antibody (Figs. 3B and C). The nucleus of yellow cells was observed at marginal cell membrane (Fig. 3E). Trypan blue did not stain most of the yellow cells (Figs. 3G and H), indicating that the cells were alive.

Changes in ratio of 3β-HSD positive cells in lymphatic fluid

The percentage of 3β-HSD positive cells to whole cells present in lymphatic fluid was significantly ($P<0.05$) higher at days 22-24 than that at the other luteal stages including mid-pregnancy (Fig. 4). Furthermore, at days 26-28 after ovulation, the ratio of 3β-HSD positive cells was significantly ($P<0.05$) higher than that at days 8-12 and 15-17 after ovulation (Fig. 4).

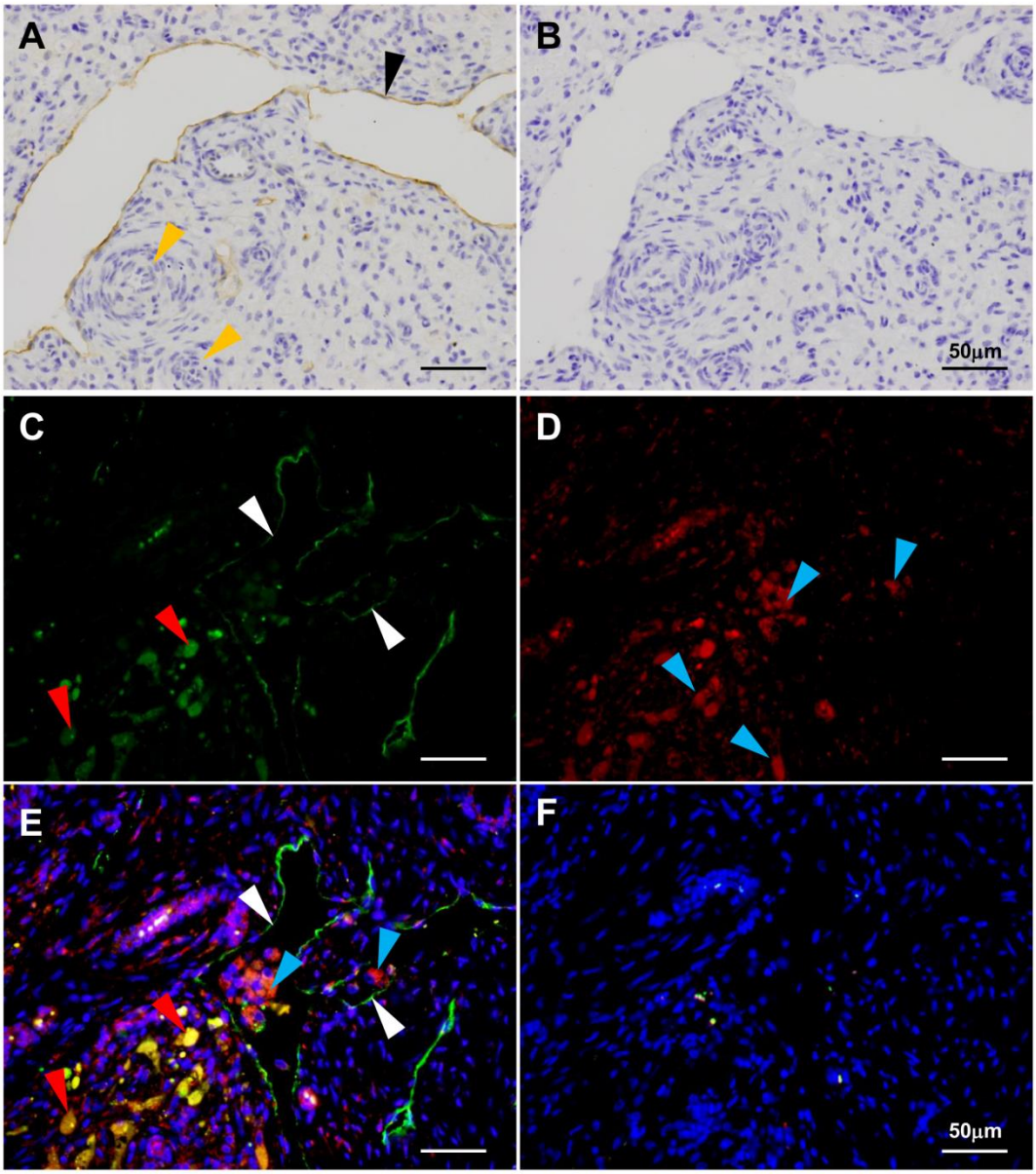

Figure 2. Immunohistochemical staining of the regressing bovine CL tissue.

A: Large lymphatic vessels (black arrowheads) were observed around arterioles (yellow arrowheads). B: Negative control. C: Lymphatic vessels were visualized by LYVE-1 antibody and goat anti rabbit IgG antibody labeled with Alexa 488 (white arrowheads). D: Steroidogenic cells were detected by 3β-HSD antibody and goat anti mouse IgG antibody labeled with Alexa 594 (blue arrowheads). E: Many 3β-HSD positive cell were observed in the lumen of LYVE-1 positive vessel (merge C and D). LYVE-1 antibody positively reacted with 3β-HSD positive cells (red arrowheads). F: Negative control. Nuclei were stained using DAPI. All scale bars, 50 μm.

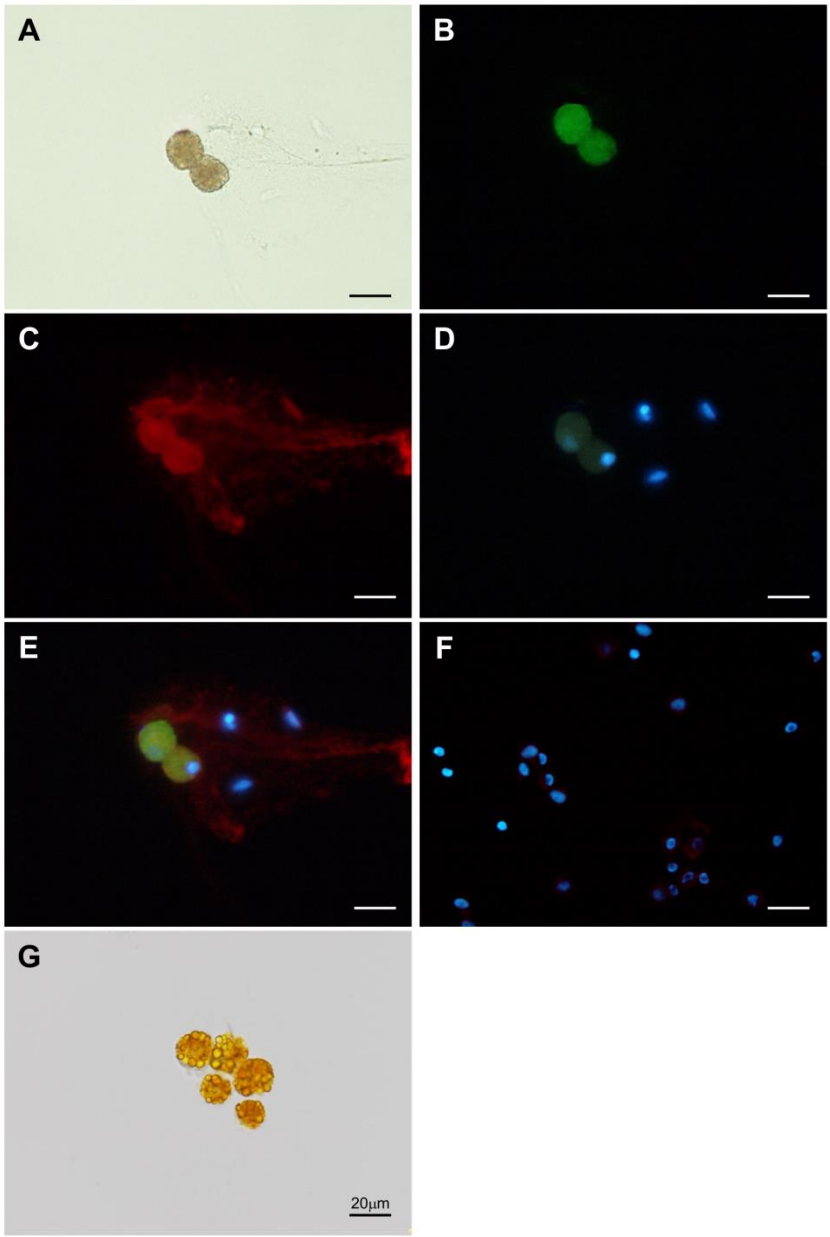

Figure 3. Staining of lymphatic fluid smear.

A: Bright field image of the cells in lymphatic fluid. B: Lipid droplets in the cells were stained by Bodipy 493/503. C: The same cells show a positive signal for 3β-HSD. D: The nuclei in the cells were visualized using DAPI. E: Merge image of B, C and D. The nucleus was located by marginal cell membrane (white arrowhead). F: Cultured bovine endometrial stromal cells were used as negative control. G: Many lipid droplets were observed as granules in cytoplasm (black arrowhead). Most of the cells in the lymphatic fluids were not stained by trypan blue solution. All scale bars, 20 μm.

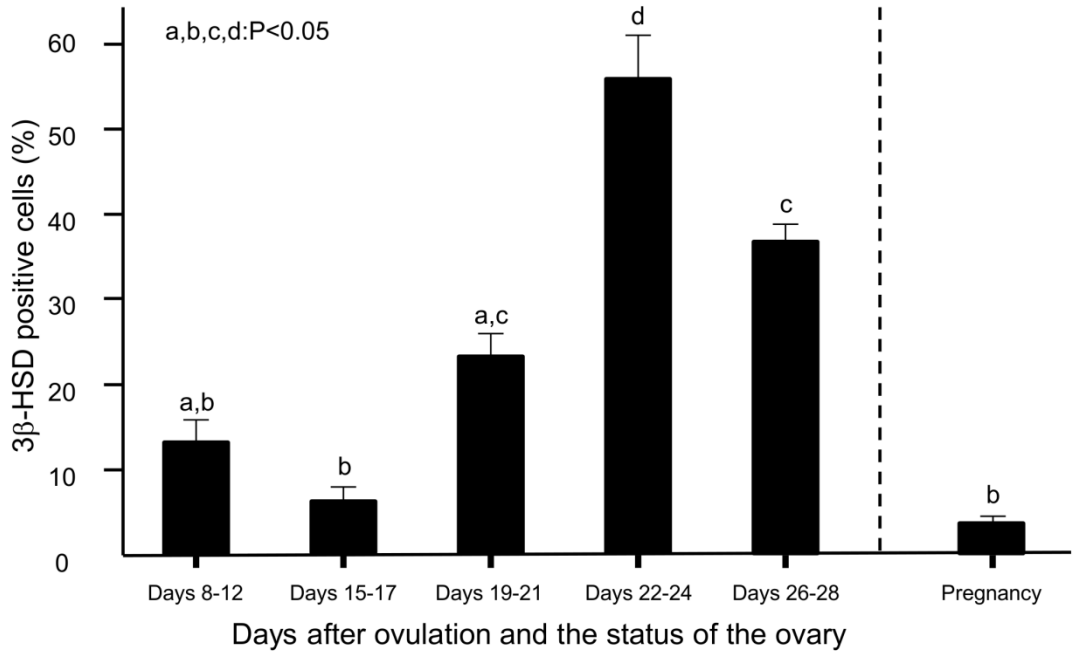

Figure 4. 3β-HSD positive cells in the lymphatic fluid during the estrous cycles and pregnancy. Different superscript letters indicate significant difference ($P<0.05$) compared with the other luteal stages as assessed by ANOVA followed by a Fisher's protected least significant difference procedure (PLSD) as a multiple comparison test (n=3/luteal stage). The percentage of 3β-HSD positive cells in the lymphatic fluid significantly increased at days 22-24 after ovulation.

DISCUSSION

The main function of the lymphatic vasculature is to transport fluid, macromolecules and cells including monocytes and lymphocytes from the tissues to the blood circulation [8]. In most cancers, the lymphatic vessels serve as the primary route for the metastatic spread of tumor cells [8]. Thus, lymphatic vessels in the CL may be a route for transporting luteal cells to outside of the CL. In the present study, we used a lymphatic endothelial hyaluronan receptor (LYVE-1) antibody and 3β-HSD antibody, a specific steroidogenic cell marker. Double-fluorescent immunohistochemistry revealed cells that react with 3β-HSD antibody in the lumen of lymphatic vessels in the regressing CL. Unexpectedly, LYVE-1 antibody reacted with 3β-HSD positive cells. LYVE-1 antibody binds to hyaluronan receptor on the lymphatic endothelial cells [18]. We are unaware of any reports that luteal cells express hyaluronan receptor. Therefore, we checked the specificity of the LYVE-1 antibody for the lymphatic endothelial cells and the specificity of the 3β-HSD antibody for luteal cells using ovarian hilus sections and mid CL sections (Fig. S1). We confirmed that the antibodies were specific to each target cell. Thus, the bovine luteal cells seem to express hyaluronan receptor. However, the role of the hyaluronan receptor in luteal cells is unclear.

Many yellow cells were found in the lymphatic fluid drained from the ovaries with a regressing CL. Similar yellow cells were dissociated from the regressing CL by collagenase (Fig. S2). These findings suggest that the regressing CL was the source of the yellow cells. These yellow cells positively reacted with 3β-HSD antibody. Luteal cells contain lipid droplets for steroid hormone synthesis[19]. Staining with Bodipy (493/503), a lipid droplets-staining regent [17], confirmed that most of the 3β-HSD positive cells found in the lymphatic fluid stored lipid droplets in their cytoplasm. Their nuclei were mostly at the edge of the cytoplasm. The nuclei of mature white adipocytes containing many lipid droplets, are also located at the edge of the cytoplasm [20]. The luteal cells of the regressing CL, which secrete only a small amount of P4, store lipid droplets in their cytoplasm [21, 22]. These findings suggest that 3β-HSD positive cells with many lipid droplets originated from the regressing CL. The diameters of most 3β-HSD positive cell in lymphatic fluid were 15-20 μm. In the luteal cells in suspension, the large luteal cells had diameters of 23-57 μm and the small luteal cells had diameters of 12.5-23 μm [19]. Based on previous findings [17,19, 20-22] and our present results, the 3β-HSD positive cells in the lymphatic vessels seem to be small luteal cells drained

from the CL.

If the steroidogenic cells found in lymphatic fluid are small luteal cells, a question remains why large luteal cells do not flow out into the lymphatic vessels. A possible explanation is that only the large luteal cells might selectively disappear from the CL by apoptosis and phagocytosis or other mechanisms. Further studies are needed to identify the steroidogenic cells drained from the ovary.

In the regressing CL, the microvasculature disappears, but the arterioles with smooth muscle remain [23]. Similarly, the large lymphatic vessels with smooth muscle remain within the regressing CL after the lymphatic capillaries disappear [8]. Luteal cells in the CL might be carried to large lymphatic vessels via an unknown pathway. Further studies are needed to understand how luteal cells enter the lymphatic vessels.

The number of the immune cells in the bovine CL is reported to increase during luteolysis [6]. However, we are unaware of any reports on the number of immune cells in lymphatic fluid drained from the CL. The number of these cells might also increase during luteolysis. In fact, in the present study, the number of 3β-HSD negative cells (which may be immune cells) increased during luteolysis, and the number of 3β-HSD positive cells increased during luteolysis as well. However, since the ratio of 3β-HSD positive cells increased during luteolysis, the number of 3β-HSD positive cells seems to increase more than that of 3β-HSD negative cells.

In the present study, the percentage of 3β-HSD positive cells in the lymphatic fluid was higher at days 22-24 and days 26-28 after ovulation than at other luteal stages, indicating that the outflow of steroidogenic cells to lymphatic vessels increases after the start of the next estrous cycle. It has been reported that bovine CL tissue does not disappear completely before the next ovulation, and that the regressing CL from the previous estrous cycle remains about at 20% of its volume compared with the size of the mid CL [3]. Indeed, the regressing CL was observed on the surface of the ovaries during days 22-28 after ovulation in the present study. Therefore, the CL seems to disappear completely from the ovaries around days 26-28 after ovulation. In this study, the ratio of 3β-HSD positive cells was less at days 26-28 than at days 22-24. These findings suggest that the possible outflow of steroidogenic cells from the CL to the lymphatic vessels starts at the regressing luteal stage (days 19-21) and continues until around day 30 after ovulation. The outflow of steroidogenic cells via lymphatic vessels appears to engage in complete disappearance of the CL from the ovary. Interestingly, some 3β-HSD positive

cells were found in lymphatic fluid drained from the ovary with the pregnant CL, and the ratio of these cells was less than 10%. The ratio of 3β-HSD positive cells was similar to that at days 8-12 (mid luteal stage) and 15-17 (late luteal stage). It is unclear why steroidogenic cells were drained from the active CL before the start of structural luteolysis. A possible explanation is that cells are drained from active tissue as cell turnover.

It takes 4-5 days to reduce the size of the CL after spontaneous PGF2α secretion from the uterus [3]. On the other hand, the volume of the CL decreased to less than half of its original size 24 h after PGF2α administration on Day 10 post ovulation [7]. However, the number of macrophages observed within the regressing CL during spontaneous and PGF2α-induced luteolysis is almost same [6]. Hence, the mechanism underlying the rapid structural luteolysis induced by PGF2α administration is unclear. We speculate that the number of luteal cells drained from the CL is greater during luteolysis induced by PGF2α administration than during spontaneous luteolysis. Further *in vivo* studies are needed to test this hypothesis.

Our results show that live steroidogenic cells are in the lymphatic vessels drained from the CL. These findings suggest that structural luteolysis involves not only apoptosis of luteal cells and phagocytosis, but also an outflow of luteal cells from the CL to the lymphatic vessels. This mechanism may ensure the definitive disappearance of the CL tissue during structural luteolysis. Possible mechanisms of structural luteolysis via the lymphatic vessels are shown in Figure 5.

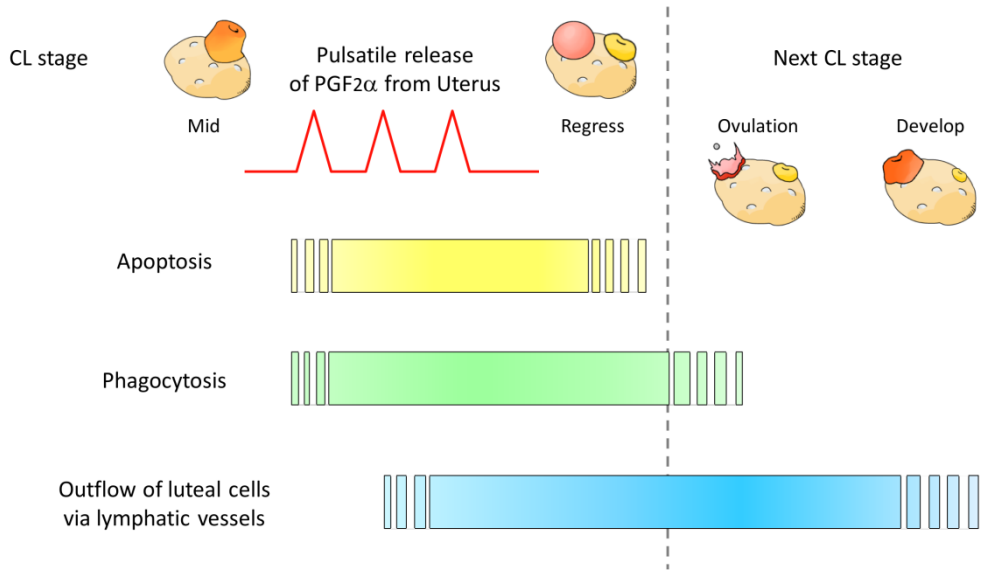

Figure 5. Possible mechanisms of structural luteolysis via lymphatic vessels. Bovine spontaneous luteolysis is caused by PGF2α from the uterus. During structural luteolysis, luteal cells are killed by apoptosis, and macrophages simultaneously infiltrate into the CL to remove luteal cells by phagocytosis. Immediately after starting phagocytosis, luteal cells start flowing into the lymphatic vessels. Luteolysis proceeds to a phase of next ovulation. After ovulation, the outflow of the luteal cells continues, and ensures the definitive disappearance of the CL tissue from the ovary.

SUMMARY

In mammals, the corpus luteum (CL) is an essential endocrine gland for the establishment and maintenance of pregnancy. If pregnancy is not established, the CL regresses and disappears rapidly from the ovary. A possible explanation for the rapid disappearance of the CL is that luteal cells are transported from the ovary via lymphatic vessels. Here, we report the presence of cells positive for 3β-hydroxysteroid dehydrogenase (3β-HSD), an enzyme involved in progesterone synthesis, in the lumen of lymphatic vessels at the regressing luteal stage and in the lymphatic fluid collected from the ovarian pedicle ipsilateral to the regressing CL. The 3β-HSD positive cells were alive and contained lipid droplets. The 3β-HSD positive cells in the lymphatic fluid were most abundant at days 22-24 after ovulation. These findings show that live steroidogenic cells are in the lymphatic vessels drained from the CL. The outflow of steroidogenic cells starts at the regressing luteal stage and continues after next ovulation. The overall findings suggest that the complete disappearance of the CL during luteolysis is involved in the outflow of luteal cells from the CL via ovarian lymphatic vessels.

CHAPTER 2
How luteal cells were detached from the CL?

INTRODUCTION

The outflow of luteal cells during luteolysis was presented in chapter 1. However, the mechanisms regulating the outflow of luteal cells from the CL are unclear. Matrix metalloproteinases (MMPs) are a family of structurally-related proteins that degrade the extracellular matrix (ECM) and basal membrane [24]. The ECM, besides providing structural support between cells, has been implicated in modulating cell processes, such as differentiation, migration, gene expression and apoptosis [24, 25]. In cancer metastasis, MMPs are required for cancer cell to degrade ECM and intravasation at nearby blood vessels or lymphatic vessels [26-28]. In luteal cells, ECM degradation by MMPs induced changes in the mRNA expressions of luteinizing hormone receptor, low density lipoprotein receptor and 3β-hydroxy steroid dehydrogenase which are required factors to produce steroid hormones in luteal cells [29]. Hence, although these changes mediated by MMPs have been suggested to be involved in the loss of capacity of luteal tissue to synthesize progesterone during luteolysis, but the roles of MMPs in structural luteolysis are unclear.

Luteal cells that flow out to the lymphatic vessels during structural luteolysis must be detached from the CL tissue. In the bovine CL tissue, MMP-1, 2, 9 and 14 increase drastically during luteolysis induced by prostaglandin F2α (PGF) injection [30]. The authors implied that the main source of MMP-1 and -9 in the CL tissue is immune cells invading the CL during luteolysis. We hypothesized that luteolytic factors regulate the productions of MMPs in luteal cells during luteolysis, and that MMPs secreted by luteal cells break down the ECM surrounding luteal cells in the same way that MMPs secreted by cancer cells break down the ECM in metastasis. To test this hypothesis, we investigated the effects of three factors that are known to induce luteolysis (prostaglandin F2α (PGF), interferon γ (IFNG) and tumor necrosis factor α (TNF) [2]) on the mRNA expressions of four MMPs involved in degrading collagen and basal membrane in cultured luteal cell.

MATERIALS AND METHODS

Collection of Bovine Corpora Lutea

Ethics Statement

In this study, we did not perform any animal experiments. The ovaries were collected from non-pregnant Holstein cows at a local abattoir (Tsuyama Meat Center) in accordance with protocols approved by the local institutional animal care committee. All the samples and data analyzed in the present study were obtained with the permission of the above center.

Ovaries with CLs at the mid luteal stage were collected at a local abattoir within 10–20 min after exsanguination. The luteal stage was classified by macroscopic observation of the ovary and uterus [13, 14]. For cell culture experiments, ovaries with the mid-CL (Days 8–12 of the estrous cycle) were submerged in ice-cold physiological saline and transported to the laboratory.

Cell Isolation

Luteal cells were obtained as described previously [31]. Briefly, mid-CL tissue from four cows was enzymatically dissociated, and the resulting cell suspensions were centrifuged (5 min at 50x*g*) three times to separate the luteal cells (pellet) from endothelial cells and other types of luteal non-steroidogenic cells (supernatant). The dissociated luteal cells were suspended in culture medium (Dulbecco's Modified Eagle's Medium/Nutrient Mixture F-12 Ham (D/F, 1:1, v/v; no. D8900; Sigma–Aldrich Inc., St. Louis, MO, USA) containing 5% calf serum (no. 16170-078; Life Technologies Inc., Grand Island, NY, USA) and 20 μg/ml gentamicin (no. 15750-060; Life Technologies), and cultured with 5% CO_2 in air. Cell viability was greater than 80%, as assessed by trypan blue exclusion. The cells in the cell suspension after centrifugation consisted of about 70% small luteal cells, 20% large luteal cells, 10% endothelial cells or fibrocytes, and no erythrocytes.

Cell Culture

The dispersed luteal cells were seeded at 2.0×10^5 viable cells in 1 ml in 24-well culture dishes (no. 662160; Greiner Bio-One, Frickenhausen, Germany) to evaluate mRNA expression. The cultures were kept in a humidified atmosphere of 5%

CO_2 in air at 38°C in an N_2–O_2–CO_2-regulated incubator (no. BNP-110; ESPEC Corp., Osaka, Japan). After 24 h of culture, medium was replaced with fresh medium containing 0.1% BSA (no. 15408; Roche Diagnostics, Mannhein, Germany), 5 ng/ml sodium selenite (no. S5261; Sigma–Aldrich), 5 μg/ml holo- transferrin (no. T3400; Sigma–Aldrich), 0.01, 0.1, 1 μM PGF (no. 16010; Cayman chemical, MI, USA) or 0.05, 0.5, 5 nM TNF (Dainippon Pharmaceutical, Osaka, Japan) or 0.05, 0.5. 0.5 nM IFNG (Kindly donated by Dr. S. Inumaru, NIAH, Ibaraki, Japan) for 24 h. Concentration of PGF, IFNG and TNF for combination treatment were determined based on the those which were most effective to the expression of *MMPs* mRNA in single treatment of PGF, IFNG and TNF. The luteal cells were also exposed to 1 μM PGF in combination with 5 nM IFNG or 5 nM TNF, 5 nM IFNG in combination with 5 nM TNF, 1μM PGF in combination with 5 nM IFNG and 5 nM TNF for 24 h.

RNA Isolation and cDNA Synthesis

Total RNA was extracted from CL tissues and cells using TRIzol regent (no. 15596-026; Invitrogen, Carlsbad, CA, USA) according to the manufacturer's directions. One μg of each total RNA was reverse transcribed using a ThermoScript RT-PCR System (no. 11146-016; Invitrogen).

Quantitative PCR (Real-Time PCR)

Ten percent of the reaction mixture was used in each PCR using specific primers for MMPs (Table 1). mRNA expression was quantified by iQ SYBR Green Supermix (no. 170-8880; Bio-Rad Laboratories, CA, USA) starting with 2 ng of reverse-transcribed total RNA. The PCR contents were 95 C for 15 min, followed by 45 cycles of 94 C for 15 sec, 55 C for 30 sec and 72 C for 30 sec. Use of the QuantiTect^{TM} SYBR Green PCR system at elevated temperatures resulted in reliable and sensitive quantification of the RT-PCR products with high linearity. The relative level of expression of each mRNA was analyzed by the 2- $^{\Delta\Delta}$CT method [32, 33].

Statistical analysis

All experimental data are shown as the mean±SEM. The statistical significances of differences in the expression of MMPs mRNA were assessed by one-way ANOVA followed by a Tukey's multiple comparisons test or Kluskal-Wallis

test followed by Dunn's multiple comparisons test, and Student's t-test or Mann Whitney test based on test for homogeneity of variance. Statistical analyses used in each experiment were described in legends of Figures.

Target	Primer	Sequence (5'-3')	Accession no.	Product (bp)
MMP-1	Forward	AGGTGCAGGTATCGGAGGAG	NM174112	275
	Reverse	CACACACTTCTGGGGTTTGG		
MMP-2	Forward	GGCATCTCTCAGATCCGTGG	NM174745.2	155
	Reverse	TGTGGGTCTTCGTACACAGC		
MMP-9	Forward	CTAGTTGGGATCCGGCAGAC	NM174744	128
	Reverse	CTAGTTGGGATCCGGCAGAC		
MMP-14	Forward	GAGTGACAGGCAAGGCTGAT	NM174390.2	200
	Reverse	AAATGTGGCATACTCGCCCA		
ACTB	Forward	CAGCAAGCAGGAGTACGATG	AY141970	137
	Reverse	AGCCATGCCAATCTCATCTC		

Table. 1 Primers for MMPs used in quantitative RT-PCR

RESULTS

Effects of single treatment of PGF, IFNG or TNF on *MMPs* mRNA expression

MMP-1 mRNA expression in cultured luteal cells was stimulated by PGF and IFNG (Fig. 6A and B). The levels of *MMP-2* and *MMP-9* mRNA expression were not affected by PGF, IFNG and TNF (Fig. 6D-I). IFNG suppressed *MMP-14* mRNA expression (Fig. 6K).

Effects of combination treatment of PGF, IFNG and/or TNF on *MMPs* mRNA expression

Based on the above results, 1 μM PGF, 5 nM IFNG and 5 nM TNF were used in this experiment. *MMP-1* mRNA expression was stimulated more by PGF in combination with IFNG than by each treatment alone (Fig. 7A). IFNG in combination with or without PGF and TNF decreased *MMP-2* and *MMP-14* mRNA expression (MMP-2: Fig. 8A and C) (MMP-14: Fig. 10A, C and D). PGF in combination with IFNG increased *MMP-9* mRNA expression (Fig. 9A), whereas PGF in combination with IFNG and TNF did not affect *MMP-9* mRNA expression (Fig. 9D).

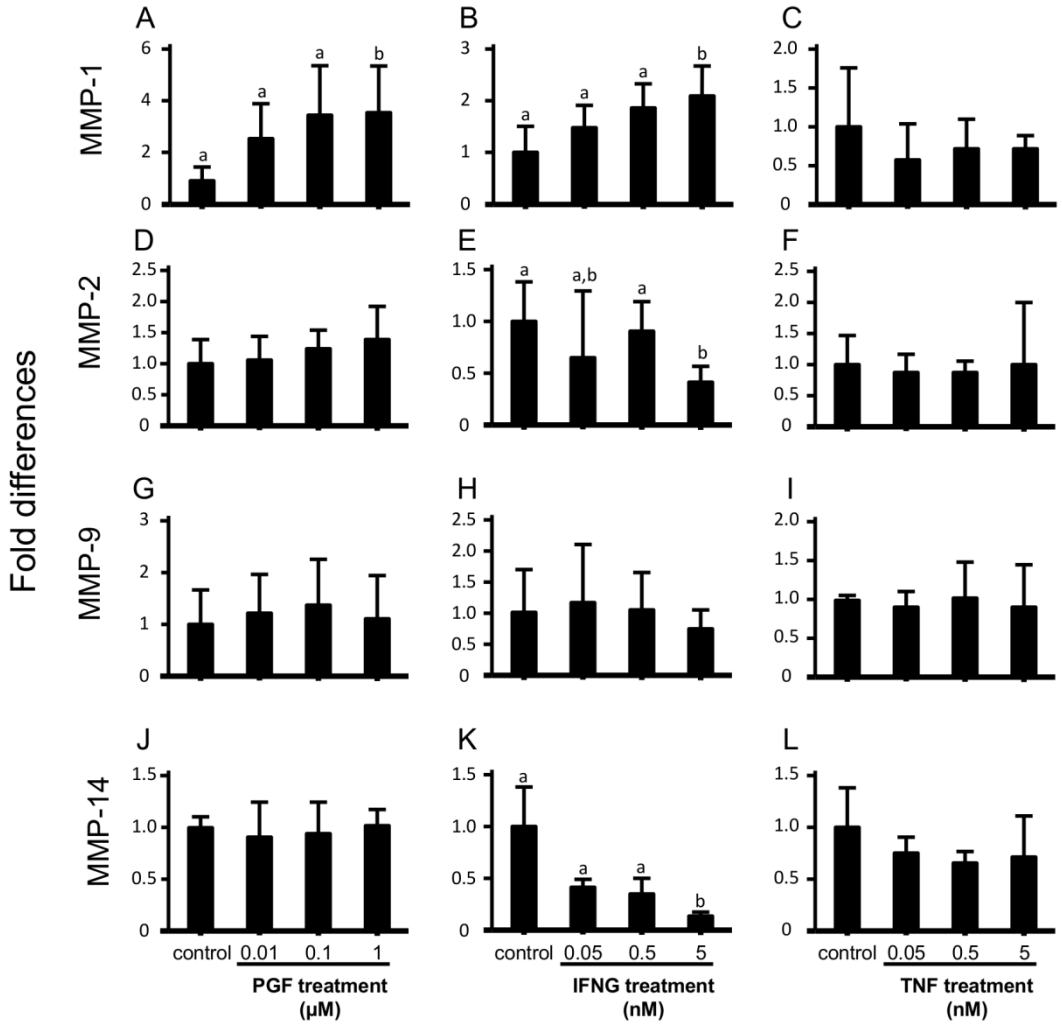

Figure 6. Regulation of *MMsP* mRNA expressions in cultured bovine luteal cells following single treatments with different concentrations of PGF, IFNG and TNF for 24h.

(A-C) MMP-1. (D-F) MMP-2. (G-I) MMP-9. (J-L) MMP-14. Different superscript letters indicate significant difference ($P<0.05$) compared with other columns as assessed by Kluskal-Wallis test followed by Dunn's multiple comparisons test (A and K) or one-way ANOVA followed by a Tukey's multiple comparisons test (B-J and L). Data are the mean+SEM for 4 experiments.

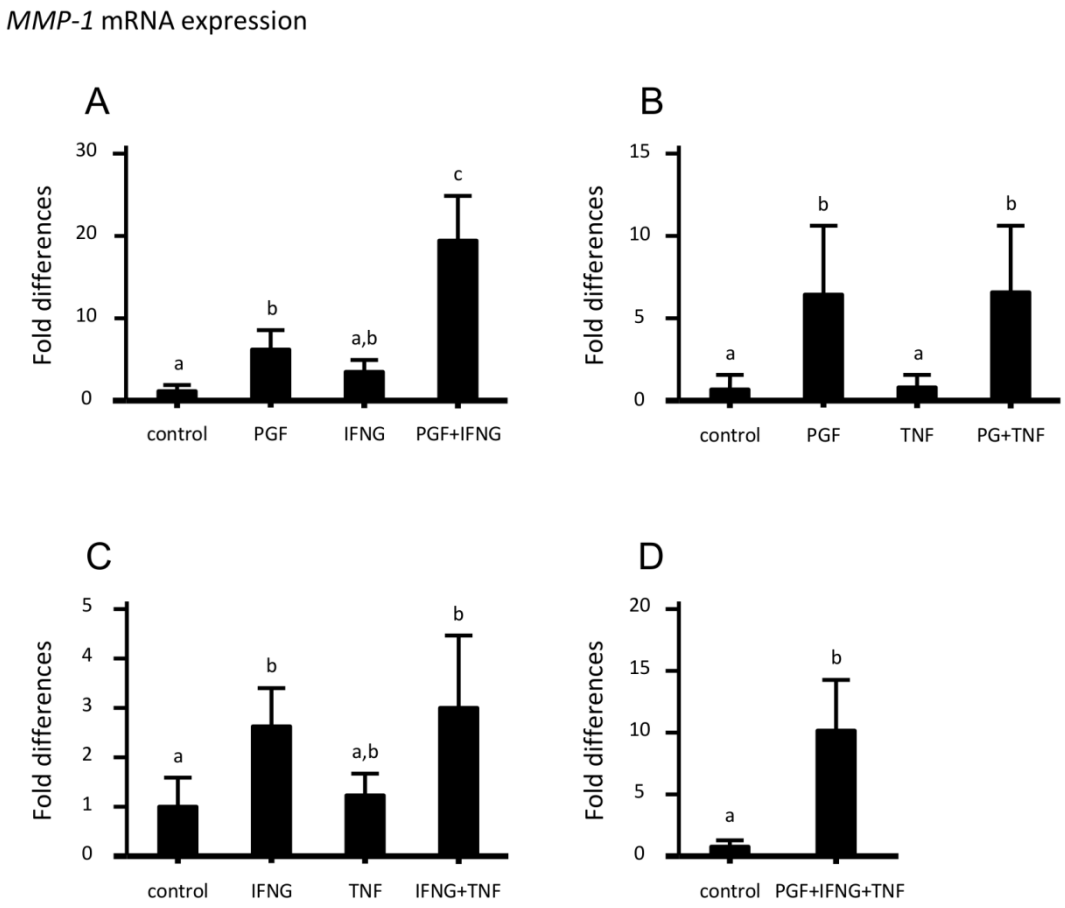

Figure 7. Regulation of *MMP-1* mRNA expression in cultured bovine luteal cells following combination treatment by 1 μM PGF, 5 nM IFNG and 5 nM TNF for 24 h.

(A) PGF in combination with IFNG significantly stimulated the expression of MMP-1 mRNA in luteal cells compared with single treatment with PGF or IFNG. (B, C, D) The other results were same as those induced by single dose treatments. Different superscript letters indicate significant difference ($P<0.05$) compared with other columns as assessed by Kluskal-Wallis test followed by Dunn's multiple comparisons test (A, B, C) and Mann Whitney test (D). Data are the mean±SEM for 4 experiments.

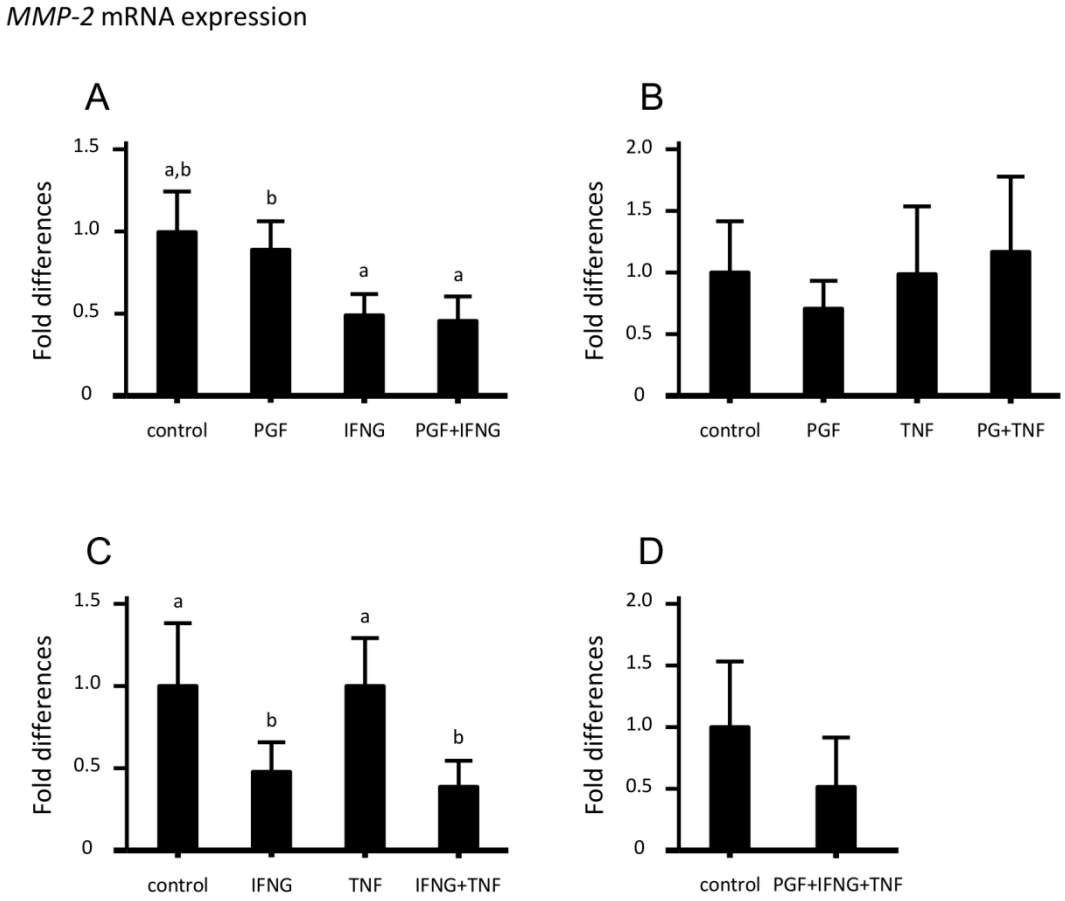

Figure 8. Regulation of *MMP-2* mRNA expression in cultured bovine luteal cells following combination treatment by 1 μM PGF, 5 nM IFNG and 5 nM TNF for 24 h.

(A, B, C, D) All changes in *MMP-2* mRNA expression induced by combination treatments were the same as those induced by single dose treatment. Different superscript letters indicate significant difference ($P<0.05$) compared with other culms as assessed by repeated measures ANOVA followed by a Tukey's multiple comparisons test (A, B, C) or Student's t-test (D). Data are the mean±SEM for 4 experiments.

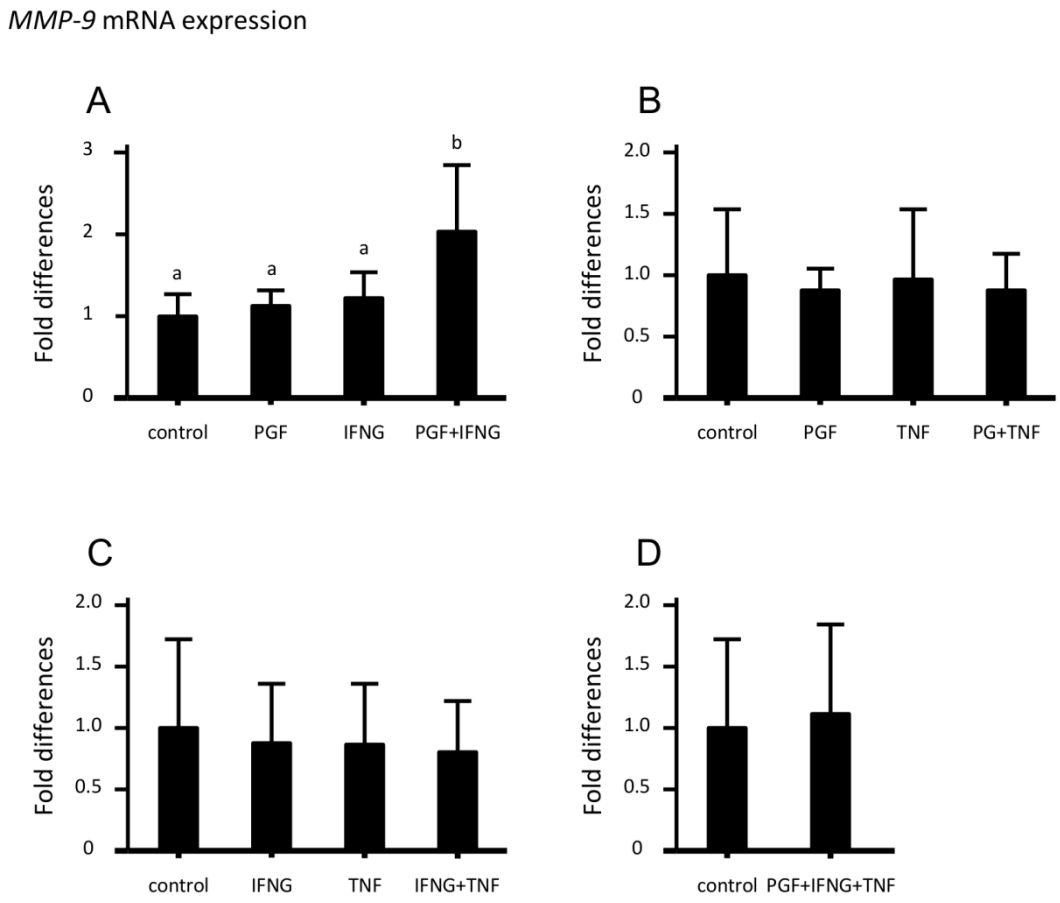

Figure 9. Regulation of *MMP-9* mRNA expression in cultured bovine luteal cells following combination treatment by 1 μM PGF, 5 nM IFNG and 5 nM TNF for 24 h.

(A) PGF in combination with IFNG significantly stimulated MMP-9 mRNA expression in luteal cells compared with that in control and single treatment of PGF or IFNG. (B, C) PGF in combination with TNF and IFNG in combination with TNF did not affect the MMP-9 mRNA expression. (D) PGF in combination with IFNG and TNF did not stimulate MMP-9 mRNA expression. Different superscript letters indicate significant difference ($P<0.05$) compared with other columns as assessed by one-way ANOVA followed by a Tukey's multiple comparisons test (A, B, C) and Student's t-test (D). Data are the mean±SEM for 4 experiments.

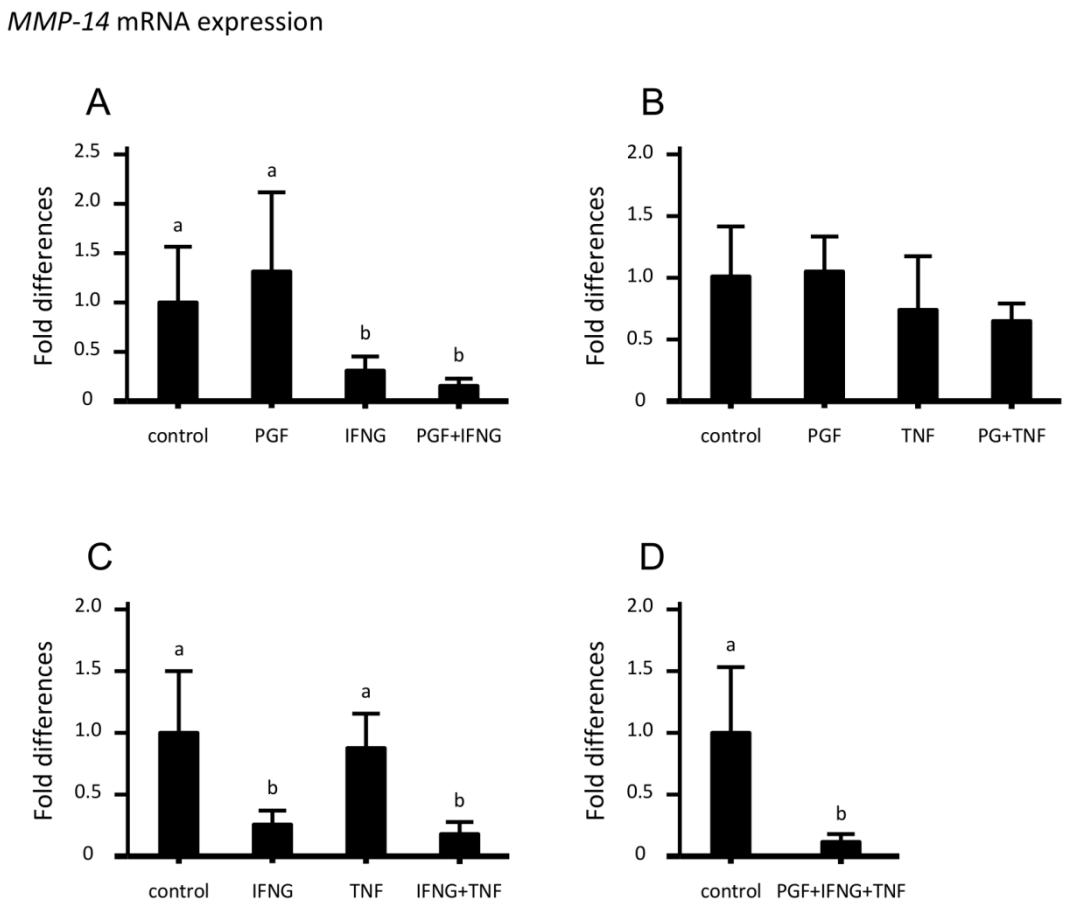

Figure 10. Regulation of *MMP-14* mRNA expression in cultured bovine luteal cells following combination treatment by 1 µM PGF, 5 nM IFNG and 5 nM TNF for 24 h.

(A) PGF in combination with INFG suppressed the expression of MMP-14 mRNA. (B) PGF in combination TNF did not affect MMP-14 mRNA expression. (C) IFNG in combination with TNF suppressed the expression of MMP-14 mRNA. (D) PGF in combination with IFNG and TNF suppressed MMP-14 mRNA expression. Different superscript letters indicate significant difference ($P<0.05$) compared with other columns as assessed by Kluskal-Wallis test followed by Dunn's multiple comparisons test (A, C) or one-way ANOVA followed by a Tukey's multiple comparisons test (B) and Mann Whitney test (D). Data are the mean±SEM for 4 experiments.

DISCUSSION

The preceding results confirmed that *MMP-1, -2, -9* and *-14* mRNA are expressed in cultured bovine luteal cells. The expression of *MMP-1, 2, 9* and *14* mRNA increased during luteolysis. These MMPs were previously found to be involved in functional luteolysis [29, 30, 34, 35]. PGF secreted by the uterus is a trigger that induces luteolysis in cow. IFNG and TNF, which are secreted by macrophages that invade CL, are also involved in inducing luteolysis [1, 2, 6, 36]. Until now, immune cells infiltrating the regressing CL were considered as the main source of *MMPs* during luteolysis [30]. In the present study, PGF and IFNG stimulated the expression of *MMP-1* and *-9* mRNA in cultured bovine luteal cells, which suggests that luteal cells are also important sources of MMPs, especially MMP-1, during luteolysis.

During structural luteolysis, luteal cells flow out of the CL via lymphatic vessels drained from the CL [37]. Luteal cells have to be detached from the CL tissue to flow out to the lymphatic vessels. The CL tissue is composed of collagens which are the main components of ECM, and the predominant luteal collagen is collagen type I [38, 39]. MMP-1, secreted from cells and MMP-14 anchored to plasma membrane, have the ability to cleave collagen types I, II and III [40, 41]. In the present study, PGF in combination with IFNG strongly stimulated *MMP-1* mRNA expression in cultured luteal cells, which suggests that MMP-1 secreted by luteal cells degrades ECM surrounding luteal cell and promotes the detachment of luteal cells from the CL tissue during luteolysis.

Since MMP-14 expresses is expressed on the cell membrane of large luteal cells [30], MMP-14 may assist the outflow of luteal cells by digesting the pericellular ECM. We expected that luteolytic factors such as PGF, IFNG and TNF up-regulate *MMP-14* mRNA expression in luteal cells. However, *MMP-14* mRNA did not change by any dose of these factors. On the other hand, IFNG strongly suppressed the expression of *MMP-14* mRNA in luteal cells. *MMP-14* mRNA expression in the CL tissue has been reported to increase during luteolysis [30]. Our results suggest that luteal cells are not involved in the increase of *MMP-14* mRNA expression during luteolysis. In cancer cell invasion, MMP-14 is localized at the front of migrating cells and degrades ECM [42, 43]. Therefore, we expected that luteal cells migrate by MMP-14 and enter the luteal lymphatic vessels. However, the present results contradict this hypothesis. Another explanation for the movement of luteal cell could be that luteal cells detached

from the CL tissue by MMP-1 are transported by interstitial fluids that come from blood plasma and flow into the lymphatic vessels. However, blood flow in the CL decreases during luteolysis [7]. Further study is needed to clarify how luteal cells move in the CL tissue to the lymphatic vessels.

Basal membrane, which provides structural supports to the wall of blood vessels, is degraded by MMP-2 and MMP-9 [41]. Basal membrane has been found surrounding the lymphatic vessels that differentiated from vein [8, 44, 45]. Immune cells such as lymphocytes and macrophages invading the CL migrate into the lymphatic node from the CL during luteolysis [46]. Therefore, it is necessary process to degrade basal membrane when immune cells enter the lymphatic vessels. In this study, IFNG suppressed *MMP-2* mRNA expression, while PGF in combination with IFNG induced *MMP-9* mRNA expression. Interestingly, PGF in combination with IFNG and TNF eliminated the effect of PGF in combination with IFNG on the expression of *MMP-9* mRNA. MMP-2 and MMP-9 secreted by luteal cells may support immune cells to enter the lymphatic vessels by degrade basal membrane, and these expressions in luteal cells may to be regulated by macrophages which have capacity to secrete IFNG and TNF.

During luteolysis induced by PGF administration on Day 10 post ovulation in *vivo*, the volume of the CL decreases to less than half of its original size in 24 h [7]. Recently, we demonstrated the involvement of lymphatic vessels in this rapid shrinking of the CL [37], and the present findings seem to support this idea. PGF administration seems to up-regulate the synthesis of MMP-1 in luteal cells. MMP-1 may degrade the ECM surrounding luteal cells, resulting in the detachment of the luteal cells from the CL tissue and their outflow through the lymphatic vessels.

MMP-1, 2 and 9 are secreted as inactivate forms (pro-MMPs) [47]. Plasmin activated from plasminogen (PLG) by urokinase plasminogen activator (uPA) cleaves pro-MMP-1 and 9, while pro-MMP-2 is activated by MMP-14 on the cell surface [47]. In this study, the expressions of *PLG* and *uPA* mRNA in luteal cells and the effects of PGF, IFNG and TNF on those mRNA expressions were also investigated. Only *uPA* mRNA expression was confirmed in luteal cells. However, PGF, IFNG and TNF did not affect the level of *uPA* mRNA expression (data not shown). T-lymphocytes and macrophages producing uPA are known to invade the CL during luteolysis [6, 48, 49]. Therefore it is possible that plasminogen supplied from blood plasma is cleaved to plasmin by uPA. Then, plasmin may cleave pro-MMP-1 and pro-MMP-9 produced by luteal cells.

In summary, our results show that luteolytic factors such as PGF and IFNG regulate the expression of *MMPs* mRNA in luteal cells (Table 2). The overall findings suggest that MMPs secreted by luteal cells degrade the ECM surrounding luteal cells during luteolysis. Degradation of the ECM may be the first step for luteal cells to flow out from the CL into the lymphatic vessels.

Luteolytic factor	Target mRNA			
	MMP-1	MMP-2	MMP-9	MMP-14
PGF	↑	→	→	→
IFNG	↑	↓	→	↓
TNF α	→	→	→	→
PGF+IFNG	↑ ↑	↓	↑	↓ ↓
PGF+TNF α	↑	→	→	→
IFNG+TNF α	↑	↓	→	↓ ↓
PGF+INFG+TNF α	↑ ↑	↓	→	↓ ↓

Table 2. Effect of luteolytic factors on *MMPs* mRNA expression in bovine luteal cells.

The present study suggested that PGF and IFNG are the main factors to regulate the expression of *MMPs* mRNA in bovine luteal cells.

SUMMARY

Luteal cells flow out from the ovary via lymphatic vessels during luteolysis. However, the regulatory mechanisms of the outflow of luteal cells are not known. To test the hypothesis that matrix metalloproteinases (MMPs) are involved in the outflow, we investigated the effects of luteolytic factors such as prostaglandin F2α (PGF), interferon γ (IFNG) and tumor necrosis factor α (TNF) on the mRNA expressions of MMPs in cultured luteal cells. Luteal cells obtained from the CL at the mid-luteal stage (days 8-12 after ovulation) were cultured with PGF (0.01, 0.1, 1 μM), IFNG (0.05, 0.5, 5 nM) and TNF (0.05, 0.5, 0.5 nM) alone or in combination for 24 h. PGF and IFNG significantly increased the *MMP-1* mRNA. In addition, 1 μM PGF in combination with 5 nM IFNG stimulated *MMP-1* and *MMP-9* mRNA expression significantly more than did either treatment alone. In contrast, IFNG significantly decreased the levels of *MMP-2* and *MMP-14* mRNA. Five nM IFNG in combination with 5 nM TNF suppressed *MMP-14* mRNA expression significantly more than did 5 nM IFNG alone. The overall results suggest that luteal MMPs stimulated by PGF and IFNG break down extracellular matrix surrounding luteal cells, resulting in the outflow of luteal cells from the CL tissue to lymphatic vessels.

REFERENCE

[1] **Schams D, Berisha B.** Regulation of corpus luteum function in cattle--an overview. *Reprod Domest Anim* 2004; 39: 241-251.

[2] **Sugino N, Okuda K.** Species-related differences in the mechanism of apoptosis during structural luteolysis. *J Reprod Dev* 2007; 53: 977-986.

[3] **Miyamoto A, Shirasuna K, Wijayagunawardane MP, Watanabe S, Hayashi M, Yamamoto D, Matsui M, Acosta TJ.** Blood flow: a key regulatory component of corpus luteum function in the cow. *Domest Anim Endocrinol* 2005; 29: 329-339.

[4] **Hehnke KE, Christenson LK, Ford SP, Taylor M.** Macrophage infiltration into the porcine corpus luteum during prostaglandin F2 alpha-induced luteolysis. *Biol Reprod* 1994; 50: 10-15.

[5] **Pate JL, Landis Keyes P.** Immune cells in the corpus luteum: friends or foes? *Reproduction* 2001; 122: 665-676.

[6] **Penny LA, Armstrong D, Bramley TA, Webb R, Collins RA, Watson ED.** Immune cells and cytokine production in the bovine corpus luteum throughout the oestrous cycle and after induced luteolysis. *J Reprod Fertil* 1999; 115: 87-96.

[7] **Acosta TJ, Yoshizawa N, Ohtani M, Miyamoto A.** Local changes in blood flow within the early and midcycle corpus luteum after prostaglandin F(2 alpha) injection in the cow. *Biol Reprod* 2002; 66: 651-658.

[8] **Wang Y, Oliver G.** Current views on the function of the lymphatic vasculature in health and disease. *Genes Dev* 2010; 24: 2115-2126.

[9] **Brown HM, Robker RL, Russell DL.** Development and hormonal regulation of the ovarian lymphatic vasculature. *Endocrinology* 2010; 151: 5446-5455.

[10] **Nitta A, Shirasuna K, Haneda S, Matsui M, Shimizu T, Matsuyama S, Kimura K, Bollwein H, Miyamoto A.** Possible involvement of IFNT in lymphangiogenesis in the corpus luteum during the maternal recognition period in the cow. *Reproduction* 2011; 142: 879-892.

[11] **Xu F, Stouffer RL.** Existence of the lymphatic system in the primate corpus luteum. *Lymphat Res Biol* 2009; 7: 159-168.

[12] **Eley RM, Thatcher WW, Bazer FW, Wilcox CJ, Becker RB, Head HH, Adkinson RW.** Development of the conceptus in the bovine. *J Dairy Sci* 1978;

61: 467-473.

[13] **Miyamoto Y, Skarzynski DJ, Okuda K.** Is tumor necrosis factor alpha a trigger for the initiation of endometrial prostaglandin F(2alpha) release at luteolysis in cattle? *Biol Reprod* 2000; 62: 1109-1115.

[14] **Okuda K, Kito S, Sumi N, Sato K.** A study of the central cavity in the bovine corpus luteum. *Vet Rec* 1988; 123: 180-183.

[15] **Banerji S, Ni J, Wang SX, Clasper S, Su J, Tammi R, Jones M, Jackson DG.** LYVE-1, a new homologue of the CD44 glycoprotein, is a lymph-specific receptor for hyaluronan. *J Cell Biol* 1999; 144: 789-801.

[16] **Prevo R, Banerji S, Ferguson DJ, Clasper S, Jackson DG.** Mouse LYVE-1 is an endocytic receptor for hyaluronan in lymphatic endothelium. *J Biol Chem* 2001; 276: 19420-19430.

[17] **Spangenburg EE, Pratt SJ, Wohlers LM, Lovering RM.** Use of BODIPY (493/503) to visualize intramuscular lipid droplets in skeletal muscle. *J Biomed Biotechnol* 2011; 2011: 598358.

[18] **Berisha B, Schilffarth S, Kenngott R, Sinowatz F, Meyer HH, Schams D.** Expression of lymphangiogenic vascular endothelial growth factor family members in bovine corpus luteum. *Anat Histol Embryol* 2013; 42: 292-303.

[19] **Weber DM, Fields PA, Romrell LJ, Tumwasorn S, Ball BA, Drost M, Fields MJ.** Functional differences between small and large luteal cells of the late-pregnant vs. nonpregnant cow. *Biol Reprod* 1987; 37: 685-697.

[20] **Marzolla V, Armani A, Zennaro MC, Cinti F, Mammi C, Fabbri A, Rosano GM, Caprio M.** The role of the mineralocorticoid receptor in adipocyte biology and fat metabolism. *Mol Cell Endocrinol* 2012; 350: 281-288.

[21] **Deane HW, Hay MF, Moor RM, Rowson LE, Short RV.** The corpus luteum of the sheep: relationships between morphology and function during the oestrous cycle. *Acta Endocrinol (Copenh)* 1966; 51: 245-263.

[22] **Donaldson L, Hansel W.** Histological Study of Bovine Corpora Lutea. *J Dairy Sci* 1965; 48: 905-909.

[23] **Hojo T, Al-Zi'abi MO, Skarzynski DJ, Acosta TJ, Okuda K.** Changes in the vasculature of bovine corpus luteum during the estrous cycle and prostaglandin F2alpha-induced luteolysis. *J Reprod Dev* 2009; 55: 512-517.

[24] **Hulboy DL, Rudolph LA, Matrisian LM.** Matrix metalloproteinases as mediators of reproductive function. *Mol Hum Reprod* 1997; 3: 27-45.

[25] **Smith MF, McIntush EW, Ricke WA, Kojima FN, Smith GW.** Regulation of ovarian extracellular matrix remodelling by metalloproteinases and their tissue inhibitors: effects on follicular development, ovulation and luteal function. *J Reprod Fertil Suppl* 1999; 54: 367-381.

[26] **Egeblad M, Werb Z.** New functions for the matrix metalloproteinases in cancer progression. *Nat Rev Cancer* 2002; 2: 161-174.

[27] **Yang Q, Ye ZY, Zhang JX, Tao HQ, Li SG, Zhao ZS.** Expression of matrix metalloproteinase-9 mRNA and vascular endothelial growth factor protein in gastric carcinoma and its relationship to its pathological features and prognosis. *Anat Rec (Hoboken)* 2010; 293: 2012-2019.

[28] **Gialeli C, Theocharis AD, Karamanos NK.** Roles of matrix metalloproteinases in cancer progression and their pharmacological targeting. *FEBS J* 2011; 278: 16-27.

[29] **Smith MF, Ricke WA, Bakke LJ, Dow MP, Smith GW.** Ovarian tissue remodeling: role of matrix metalloproteinases and their inhibitors. *Mol Cell Endocrinol* 2002; 191: 45-56.

[30] **Kliem H, Welter H, Kraetzl WD, Steffl M, Meyer HH, Schams D, Berisha B.** Expression and localisation of extracellular matrix degrading proteases and their inhibitors during the oestrous cycle and after induced luteolysis in the bovine corpus luteum. *Reproduction* 2007; 134: 535-547.

[31] **Okuda K, Miyamoto A, Sauerwein H, Schweigert FJ, Schams D.** Evidence for oxytocin receptors in cultured bovine luteal cells. *Biol Reprod* 1992; 46: 1001-1006.

[32] **Arai M, Yoshioka S, Tasaki Y, Okuda K.** Remodeling of bovine endometrium throughout the estrous cycle. *Anim Reprod Sci* 2013; 142: 1-9.

[33] **Yoshioka S, Abe H, Sakumoto R, Okuda K.** Proliferation of luteal steroidogenic cells in cattle. *PLoS One* 2013; 8: e84186.

[34] **Ricke WA, Smith GW, McIntush EW, Smith MF.** Analysis of luteal tissue inhibitor of metalloproteinase-1, -2, and -3 during prostaglandin F(2alpha)-induced luteolysis. *Biol Reprod* 2002; 66: 1387-1394.

[35] **Towle TA, Tsang PC, Milvae RA, Newbury MK, McCracken JA.** Dynamic in vivo changes in tissue inhibitors of metalloproteinases 1 and 2, and matrix metalloproteinases 2 and 9, during prostaglandin F(2alpha)-induced luteolysis in sheep. *Biol Reprod* 2002; 66: 1515-1521.

[36] **Townson DH, O'Connor CL, Pru JK.** Expression of monocyte chemoattractant protein-1 and distribution of immune cell populations in the bovine corpus luteum throughout the estrous cycle. *Biol Reprod* 2002; 66: 361-366.

[37] **Abe H, Al-zi'abi MO, Sekizawa F, Acosta TJ, Skarzynski DJ, Okuda K.** Lymphatic involvement in the disappearance of steroidogenic cells from the corpus luteum during luteolysis. *PLoS One* 2014; 9: e88953.

[38] **Luck MR, Zhao Y.** Identification and measurement of collagen in the bovine corpus luteum and its relationship with ascorbic acid and tissue development. *J Reprod Fertil* 1993; 99: 647-652.

[39] **Irving-Rodgers HF, Roger J, Luck MR, Rodgers RJ.** Extracellular matrix of the corpus luteum. *Semin Reprod Med* 2006; 24: 242-250.

[40] **Hua H, Li M, Luo T, Yin Y, Jiang Y.** Matrix metalloproteinases in tumorigenesis: an evolving paradigm. *Cell Mol Life Sci* 2011; 68: 3853-3868.

[41] **Klein T, Bischoff R.** Physiology and pathophysiology of matrix metalloproteases. *Amino Acids* 2011; 41: 271-290.

[42] **Mori H, Tomari T, Koshikawa N, Kajita M, Itoh Y, Sato H, Tojo H, Yana I, Seiki M.** CD44 directs membrane-type 1 matrix metalloproteinase to lamellipodia by associating with its hemopexin-like domain. *EMBO J* 2002; 21: 3949-3959.

[43] **Itoh Y, Ito N, Nagase H, Evans RD, Bird SA, Seiki M.** Cell surface collagenolysis requires homodimerization of the membrane-bound collagenase MT1-MMP. *Mol Biol Cell* 2006; 17: 5390-5399.

[44] **Vainionpaa N, Butzow R, Hukkanen M, Jackson DG, Pihlajaniemi T, Sakai LY, Virtanen I.** Basement membrane protein distribution in LYVE-1-immunoreactive lymphatic vessels of normal tissues and ovarian carcinomas. *Cell Tissue Res* 2007; 328: 317-328.

[45] **Kesler CT, Liao S, Munn LL, Padera TP.** Lymphatic vessels in health and disease. *Wiley Interdiscip Rev Syst Biol Med* 2013; 5: 111-124.

[46] **Shirasuna K, Shimizu T, Matsui M, Miyamoto A.** Emerging roles of immune cells in luteal angiogenesis. *Reprod Fertil Dev* 2013; 25: 351-361.

[47] **Visse R, Nagase H.** Matrix metalloproteinases and tissue inhibitors of metalloproteinases: structure, function, and biochemistry. *Circ Res* 2003; 92: 827-839.

[48] **Welgus HG, Campbell EJ, Cury JD, Eisen AZ, Senior RM, Wilhelm SM, Goldberg GI.** Neutral metalloproteinases produced by human mononuclear phagocytes. Enzyme profile, regulation, and expression during cellular development. *J Clin Invest* 1990; 86: 1496-1502.

[49] **Sitrin RG, Todd RF, 3rd, Mizukami IF, Gross TJ, Shollenberger SB, Gyetko MR.** Cytokine-specific regulation of urokinase receptor (CD87) expression by U937 mononuclear phagocytes. *Blood* 1994; 84: 1268-1275.